Ammunition and Explosives Consequence Analysis Tool (AECAT) Enhancements to Support Naval Storage Explosive Scenarios

Neil J. McCormick, Sydney D. Ryan, and David R. Whitehouse
Lloyd's Register Advisory (Martec Limited)

Abstract

The Ammunition and Explosives Consequence Analysis Tool (AECAT) is a software tool developed to support risk-based management and explosive storage safety analyses for the Canadian Department of National Defence (DND). AECAT is a scenario-based, physically accurate explosion modelling and simulation package built upon the established Rapid City Planner (RCP) platform. RCP provides a fast and accurate blast assessment capability from one or multiple explosive munitions with calculated physics-based outcomes to predict human vulnerability and structural damage from blast and primary fragmentation effects.

The AECAT tool couples a virtual globe user interface with user-driven fusion of geospatial datasets to define storage-based explosive scenarios in a geolocated frame of reference. AECAT employs fast, first-principles computational fluid dynamics (CFD)-based calculations to evaluate consequences from complex blast wave interactions, primary fragmentation of stored ammunition and explosives, and secondary debris effects from storage magazine breakup. Three dimensional GIS-based models of the A&E storage environment are used to consider the effects of natural terrain variation and infrastructure, such as barricades and other structures, in the vicinity of the explosive event. Detailed definition of explosive stacks and storage magazine models are supported within the tool, including non-standard configurations and modelling approaches with varying levels of fidelity. The AECAT tool is deployed on standard performance laptop or desktop hardware to facilitate fast analyses on the order of minutes to hours, depending on the level of detail.

This work describes the current state of development of the AECAT software tool, with a focus on recent system enhancements to support explosive storage scenarios in multicompartment naval vessels. Modelling capabilities are demonstrated for both land- and naval-based storage scenarios, including a comparison between physics-based consequence predictions and established QD principles. A system comparison to a real-world, historical explosive event is also included.

Introduction

The Ammunition and Explosives Consequence Analysis Tool (AECAT) has been developed by Lloyd's Register (Martec Limited) to perform fast and physically accurate consequence analyses for military ammunition and explosive (A&E) storage applications. Applications of the software tool include informing on safety risks associated with A&E storage and siting, supporting domestic and expeditionary storage and licensing operations, providing validation of existing QD approaches with site-specific details not included in standard approaches, and facilitating complex analyses for marginal QD and/or non-standard storage scenarios.

The AECAT development is based upon the established Rapid City Planner (RCP) software platform, used for fast, physics-based blast and fragment effects calculations in real-world 3D environments, and introduces novel capabilities for modelling of stacked ammunition and explosives, and storage magazine fragmentation and debris effects. The system also provides an in-situ comparison of QD- and physics-based blast and fragmentation outcomes.

The AECAT system and fundamental modelling capabilities, including a system demonstration for an earth-covered magazine (ECM) scenario, are introduced and described in a previous work [1]. This paper will summarize these details for reader context but will primarily focus on preliminary validation of land-based modelling approaches and recent enhancements to support consequence analysis of naval storage scenarios.

Rapid City Planner Software Platform

Rapid City Planner (RCP) is a modelling and simulation (M&S) tool, developed by Martec Limited, that provides a fast, accurate, and easy-to-use explosive scenario outcome prediction capability [2] [3]. The tool is based on next-generation computational fluid dynamics (CFD) using shared memory processing on laptop architectures to facilitate physics-based outcomes in timeframes ranging from minutes to hours, depending on modelling fidelity. The tool uses a geographic information system (GIS)-based Virtual Globe user interface as a platform for the fusion of multiple geo-located datasets for interior and exterior environments of real-world cities. Buildings are defined using building footprints (e.g., KML or ESRI Shapefile) or detailed geo-located 3D models (e.g., KMZ, STL, OBJ, CityGML), and terrain is included in analyses using digital elevation models (DEM). Application of structure damage and human injury models provides outcomes for vulnerability and lethality assessment, including visualization in real-world coordinates using the virtual globe environment.

RCP is based on next-generation CFD combined with physical and chemical models for explosive threats. The CFD technologies have been developed since 2002 under the program name 'Chinook', a collaborative effort between Martec Limited and Defence R&D

Canada (DRDC). The blast solver capability utilizes high speed convection schemes (shock capturing methods) with an explicit time-stepping approach, with multiphase flow handled using Group Lagrangian methods. Complex blast wave phenomena are captured with this approach, including shock reflection, focusing (e.g., corners), channeling (e.g., urban canyon effects), blast clearing, as well as the detailed effects of blast initiation, detonation, reactions, and afterburning. Physical models for blast, detonation, afterburning, and target interaction have been validated using experimental data from numerous fundamental and scaled urban tests (e.g., [4] [5] [6] [7] [8]). Fast and detailed fragmentation models have been validated in [9]. The next-generation upgrades to Chinook apply a modern adaptive, Cartesian mesh grid strategy [10] in conjunction with immersed boundary methods (IBM) (e.g., [11] [12]) to perform fast blast effects computations within the RCP tool.

Historical Example (1917 Halifax Explosion)

Rapid City Planner has been used in the context of the reconstruction of an historical explosive event: the Halifax Explosion of 1917 [13] [14]. The explosion occurred in December 1917 when the French ship SS Mont-Blanc, carrying nearly 3 kilotons TNT equivalent of high explosives, collided with the Norwegian vessel SS Imo in the Halifax Harbour and caught fire. The explosion resulted in many casualties and devastation of the surrounding communities in Halifax and Dartmouth due to blast, debris, and fires.

This scenario was simulated in Rapid City Planner using fast blast effects models and historical records of the position (latitude/longitude) of the SS Mont-Blanc at the time of the explosion [13]. The 3D model consisted of the terrain variation (from a present-day digital elevation model), as well as buildings from a modern model containing footprints and heights. The effects of the water surface were not included in the analysis. Elevation variation is significant in the area of the explosion, with the Halifax Harbour roughly at sea level (0 m ASL), rising to 68 m ASL on the Halifax-side (about 600 m from ground zero) and 35 m ASL on the Dartmouth-side (about 1000 m from ground zero).

Historical records [15] were used to establish approximate regions of "totally collapsed", "burned ruins", and "badly wrecked", which were overlaid with the blast outcomes from the RCP analysis. This comparison is shown in Figure 1. In general, the RCP analysis roughly aligned with the "totally collapsed" line (dark blue) around 70 kPa overpressure, the "burned ruins" line (magenta) around 40 kPa overpressure, and the "badly wrecked" line (orange) around 15 kPa. From the built-in RCP building damage models this correlates closely to probable total destruction (69 kPa), railroad cars overturned (40 kPa), and failure of block walls (12.5 kPa) [16] [17].

The effects of the terrain and urban infrastructure are significant in this scenario and can be seen in the human injury outcome shown in Figure 2, with each isoline describing discrete vulnerability levels corresponding to incident overpressure criteria [18] [19] [20]. In a free-field scenario, these isolines would be circular and centred on the explosion location, but in this case we see blast enhancement from the inclined terrain on each side of the harbour as well as some reflected waves and shielding effects from structures in the near-field. Some local regions of higher pressure are visible in the harbour (for instance, directly to the left and right of the SS Mont-Blanc in Figure 3 3) which indicate a slight channeling effect from the surrounding terrain as well as reflections from the transition of water surface to land in the 3D model.

Figure 1. Comparison of suburban damage levels with devastated areas from [15]. *Dark blue boundaries – 'totally collapsed'; Magenta boundary – 'burned ruins'; and, Orange boundary – 'badly wrecked'.*

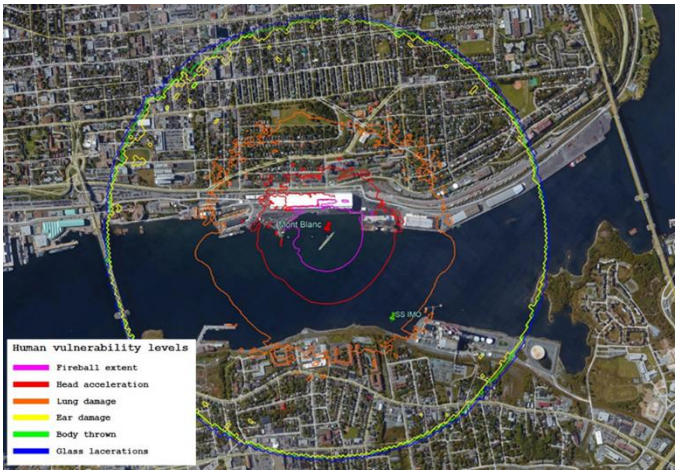

Figure 2. Rapid City Planner human vulnerability (injury) outcome for blast analysis, with each isoline corresponding to varying levels of blast overpressure.

Ammunition and Explosives Consequence Analysis Tool

The Ammunition and Explosives Consequence Analysis Tool (AECAT) has been built upon the existing RCP platform to facilitate fast and accurate consequence analyses for ammunition and explosive (A&E) storage-based explosive scenarios. The RCP platform provides a foundation of established blast analysis capabilities, including a CFD-based fast air blast solver, fast primary fragmentation and trajectory solver, and built-in structure damage and human injury outcome models. The AECAT developments build upon this platform by adding blast, fragmentation, and debris models for stacks of ammunition and storage magazine structures (including light confinement and earth-covered magazines), as well as providing a customized platform to support A&E licensing applications, including built-in QD and physics-based outcomes, geospatial data import including A&E site specification, and improved munition databases including stacking information. The resulting tool is one which provides a prediction of vulnerability and damage from an explosive event at a potential explosion site (PES) relative to exposed sites (ES), based upon first-principles blast, fragmentation, and debris

calculations, and presented with the use of QD and physics-based outcomes.

In addition to providing support for A&E risk-based licensing tasks, AECAT allows for the review of existing QD approaches with storage site-specific details not normally captured in standard licensing approaches. The modelling approaches include the effects of terrain elevation variation, nearby structures (e.g., storage magazines, explosive workshops, administrative buildings, or public developments), berms and barricades, and other relevant infrastructure. This approach is inherently well-suited in environments in which these effects have a significant impact on blast consequences and licensed quantities, as well as for storage scenarios with atypical or non-standard designs, such as magazines with partial earth covering, or temporary storage in expeditionary or deployed environments. The tool is also suitable for consequence mitigation analyses and sensitivity studies, due to the fast calculation times and the minimal effort required to modify defined scenarios. AECAT is also envisioned to be useful in situations requiring forensic analysis or event reconstruction, such as for an accidental explosion.

Software Design

The AECAT software platform consists of two primary components – the two user interfaces (Virtual Globe and Expert User Interface) including A&E-specific modelling approaches and QD outcomes for stacks and magazines, and the AECAT system databases for geospatial data, individual ammunition and explosive models, and QD functions for scenario outcomes. The software components (e.g., user interfaces) are common for any AECAT user and contain the core A&E modelling capabilities, while the database components are user-specific, and are populated with data relevant to the requirements of the user or organization.

For instance, the geospatial database contains geolocated data representing infrastructure and terrain geometry, as well as individual A&E storage site locations (e.g., individual PES or ES locations within a storage environment). The database also contains site specification information for classifying individual site locations (e.g., building/magazine types, orientation, storage information, etc.), which is used to populate the site model in AECAT. The software supports building footprint-style geometries in formats including ESRI Shapefile (SHP) and Keyhole Markup Language (KML), as well as detailed building surface models in formats including STL, Wavefront OBJ, COLLADA DAE, KMZ, and CityGML.

The A&E database contains individual models of ammunition and explosives for use in blast and fragmentation scenarios in AECAT. Entries in this database describe the geometry and material properties of individual munitions and explosives, as well as stacking parameters (e.g., orientation, spacing, and quantities) for use when defining explosive stacks. This database also contains statistical primary fragmentation distributions (from the fast fragmentation solver) for cased munitions. Individual database entries can be fully generated using the Expert User Interface (Threat GUI).

The QD database is used to define the individual QD levels (e.g., functions) used to plot scenario outcomes in AECAT. Each database entry (e.g., for a single QD level) describes the distance as a function of explosive quantity, Q (e.g., $D = f(Q)$), as well as a corresponding physical basis for that QD level relating to a calculated quantity. For instance, a given blast-based QD may correspond to a specific value of incident overpressure or impulse, or a debris/fragment-based QD may correspond to an expected fatality or injury probability. QD levels from AASTP-1 Ed. C [21] have been used during development and testing of AECAT, which separates QD levels into those for blast effects (e.g., BD) and debris/fragmentation effects (DFD). A separate database containing alternative QD levels (e.g., from another standard) can also be used.

AECAT uses the QD levels defined in the QD database along with the physical results of an A&E consequence analysis to simultaneously plot circular arc templates corresponding to the QD definition, as well as isolines corresponding to constant values of the physical basis variable and level. AECAT can also plot non-uniform QD arc templates for directional effects, such as for ECMs and barricades. This plotting capability allows for comparison of the physics based AECAT result to standard QD approaches, and can highlight differences observed from the modelling, such as the influence of terrain and surrounding infrastructure. An example of QD outcomes in AECAT is provided in Figure 3.

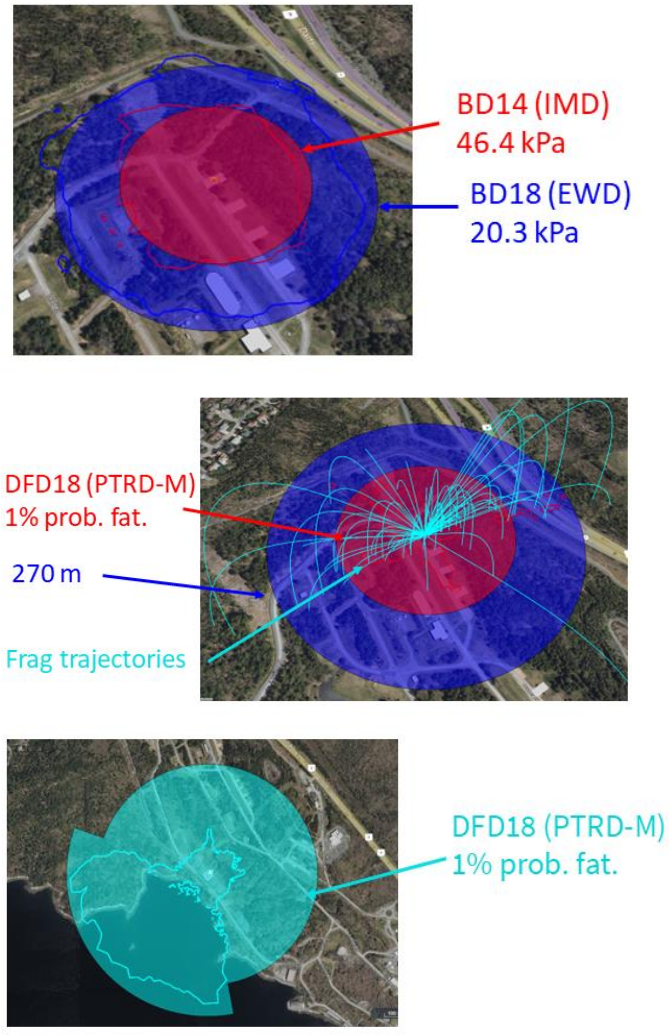

Figure 3. Example QD outcomes in AECAT for a blast effects scenario (HD 1.1) (top), a primary fragmentation scenario (HD 1.2) (middle), and an ECM magazine debris scenario (HD 1.1) with physical outcome isolines and circular arc QD templates.

Numerical Modelling Approaches

Explosive Stacks

There are strong indications from experiments that the fragmentation characteristics of stacks of weapons, detonated simultaneously or sympathetically (or any other non-design mode of initiation), differ significantly from those of a single device [22]. Due to limited experimental data, and the large number of influencing factors, there are no universally applicable rules for the differences. In fact, fragmentation codes often ignore stack effects (e.g., FragGen [23]). The purpose of this section is to describe how stack effects are incorporated into AECAT through recommended default factors to ensure results are conservative.

Fragment velocity

Fragment velocities from stacks of munitions have been seen to be up to twice as high as those from single munitions [24] [25] [26]. Although a recent review of historical test data [27] did not provide reliable data to develop a relationship between stack configuration and the increase in velocity, it is recommended that the velocity is doubled for conservatism.

Based on expert solicitation, the DDESB recommends that the velocity is increased for non-design mode initiation. Note that DDESB does not directly apply a scale factor to the velocity when calculating the Hazardous Fragment Distance (HFD) because they apply a so-called shape factor for statistics (e.g., hit probability). They do however recommend increasing the velocity for other quantities such as Maximum Fragment Distance (MFD) and perforation [27].

AECAT calculates the hit probability and other statistical quantities by directly computing all fragment trajectories. Therefore, a recommended default factor of two is applied to multiple round detonations. A smaller factor can be applied to non-design mode initiation, or specific experimental data can be inherited otherwise.

Fragment size

The number of large fragments produced by stacks of munitions is generally higher than from a single unit [22]. This effect tends to be more pronounced for weapons with small charge-to-casing mass ratios (e.g. artillery projectiles) [28] [29] than for demolition bombs [30]. The coarsening of the mass distribution may be in part due to the proximity of adjacent weapons in a closely packed stack. The radius of an isolated cased explosive may dilate to twice its initial size before breakup occurs [31] which is affected by mechanical interference between units.

Historical data suggests that stacks of munitions may produce an increase in fragment mass of up to 50% for naturally fragmenting cased explosives [32] [33]. However, tests have also indicated that fragment mass distributions are relatively similar for naturally fragmenting stacks of munitions and single units [24] [25].

Based on expert solicitation, the DDESB recommends that the mass is increased for non-design mode initiation. Note that the DDESB accounts for the increased fragment mass using the mentioned shape-factor for HFD calculations but recommends an increase for other calculations involving stacks (i.e., MFD, perforation, etc.) [27].

The fragment size of pre-formed fragmenting rounds is predesigned and will not be increased from the effects of multiple munitions. Note the velocity increase shall still be applied.

AECAT applies a recommended default increase of 50% for multiple round detonations, and 33% increase for non-design mode initiation, of naturally fragmenting munitions for conservatism unless specific experimental data is available.

Fragment count

An analysis of the results from a number of large test explosions of mass-detonating ammunition, including the ESKIMO series, has concluded that only the devices on the sides and top of a rectangular stack contribution to the far-field aerial density of hazardous fragments [34]. This means that only the items on the side of the stack facing the direction of interest and items on the top of the stack need to be considered when calculating the HFD. DDESB TP 16 [27] gives recommendations for adjusting the number of munitions considered for fragment-related stack scenarios. For stacks of munitions, the effective number of fragments is found by multiplying the number of fragments for a single item by the number of items. Although this method distinguishes between open stacks and stacks within an ECM, it does not account for directional effects associated with the orientation within the ECM which have been shown experimentally [27]. There is a lack of data on mass detonation of munitions in burial pits or underwater, and so DDESB recommends using these factors (without additional modifications) in these situations for conservatism.

AECAT has a comparable option to consider outward directed fragments from munitions on the outer faces of the stacks. Inward facing fragments are not considered in the statistical analyses or damage and injury estimation.

Verification with Continuum Breakup Model

In an effort to support these findings, a series of simulations were performed using the full-physics continuum breakup model [35] in AECAT. Each simulation contained one, or more, cylindrical munitions with a 0.4-m diameter TNT core and a 0.05-m thick steel casing. Three stack arrangements were considered: single munition, a 2x2 stack, and a 3x3 stack. The munitions were tightly packed (i.e., the spacing was equal to the munition diameter).

The continuum breakup model may predict fragment sizes using Grady theory [36]. However, as fragment sizes were not important for this analysis, a uniform diameter of 2 cm was used, which is within the lethal range (i.e., small fragments will not maintain significant kinetic energies at far distances). Figure 4 shows the fragments at 1 ms after detonation plotted with the gas phase velocity. There appears to be increases in speed for the stack configurations in localized areas influenced by the orientation of the stack. It can also be seen that a significant number of fragments are blown inward and reduce significantly in kinetic energy before propagating outward. This suggests an agreement with the ‘number of fragments’ arguments above.

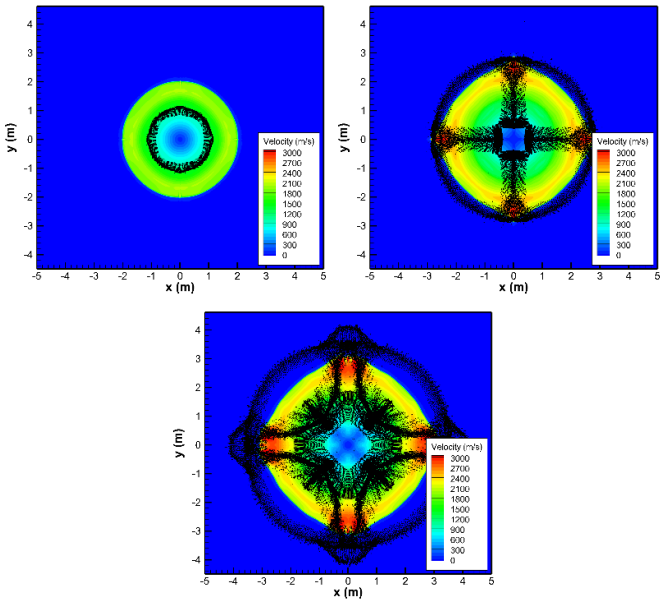

Figure 4. Contours of gas phase velocity with fragment positions (black points): single munition (top left), 2x2 stack (top right), and 3x3 stack (bottom).

Figure 5 shows the velocity of each fragment as it passes through a radial distance of 3 m, including tracer particles (zero mass) initialized within the casing material. The 2-cm sized fragments have significantly higher velocities than from the single munition. This effect is pronounced by the tracer particles which could represent smaller fragments in a naturally fragmented size distribution but is equally seen for larger fragments. The results seem to support the experimental observation of increased fragment velocities ranging to double in magnitude.

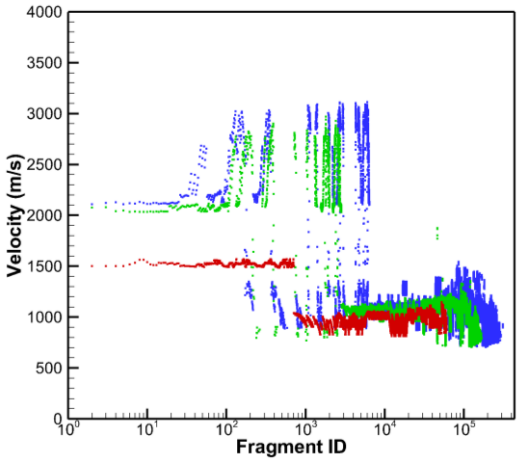

Figure 5. Velocity magnitude plotted for each fragment at a radial distance of 3 m. Red: single munition, green: 2x2 stack, blue: 3x3 stack.

Storage Magazine Debris

AECAT employs a detailed continuum breakup model for debris as well as a "fast" debris solver similar to the primary fragmentation solver. The difference between primary fragmentation and secondary debris is the reduced explosive packing density and presence of an air gap inside a magazine. Since the explosive material does not fill the interior of the magazine, it loses energy during detonation before interacting with the structure walls. This reduction in energy is inherently captured by the continuum breakup model; however, a modification to the Generalized Gurney Theory (GGT) is required to capture the effect. This section compares the debris velocity predictions for the continuum breakup model, modified GGT model and the published debris launch velocity (DLV) model described in literature. An AECAT user has the choice to select one of these velocity models or input a user-defined velocity if known from experimental measurements.

Model Descriptions

The Continuum breakup model employs a full-physics, first principles CFD approach including detonation of the unreacted explosive material, shock wave propagation and expansion [35]. The structural material is modeled as an Eulerian material using a Hugoniot Mie-Gruneisen equation of state (EOS). Tracer particles are used to monitor the strain on the structure until a failure criterion is met. At this point, the structure material is converted into fragments and subsequently tracked in a Lagrangian frame of reference. The continuum breakup model is able to capture the directional effects (e.g. non-uniform magazine wall debris launch velocity) resulting in the location and spacing of the munitions inside the structure. For this analysis, this model shall be considered the most trusted and the baseline for comparisons.

The Generalized 3D Gurney model builds on Gurney theory and assumes an instantaneous detonation of the entire explosive charge [37]. This model is widely accepted for estimating explosively driven metal fragments and has seen much success in Rapid City Planner for modelling high explosives. The 3D Gurney model is also able to approximate the directional effects and non-uniform magazine wall velocities resulting from the magazine structural composition and munition positioning within the structure. Further, a slight degree of randomness is also applied to each debris launch angle to account for inherent uncertainty in the breakup and launch mechanics. To treat the air gap, the 3D Gurney model has been adapted to explosively driven magazine debris by defining a Gurney velocity value for the airspace equal to the mass averaged Gurney velocity of the explosive material within the magazine structure.

The Debris Launch Velocity (DLV) model is an empirical model [38] [39] based on a large amount of slab launch tests. The model provides a uniform debris velocity based on the net equivalent charge (NEQ), magazine internal volume, wall density and thickness. There have been attempts to quantify the launch angle of the debris relative to the wall normal direction [40] [41], but they have not been implemented into AECAT. Instead, AECAT relies on the structure normal direction and applies a degree of randomness when assigning the launch angle in its DLV mode. This model does not account for munition positioning within the structure as with the 3D Gurney model approach. Beyond the slight increase in wall thickness on wall edges, the DLV does not have spatial dependencies or directional effects based on internal loading.

Model Verification Test Scenario

A standard ISO container was used to compare the three models. The dimensions of the ISO container were 6 m in length, 2.6 m in width, and 2.4 m in height. The wall thickness of the ISO container was 5 cm which is thicker than a standard ISO container to avoid unachievable grid resolution for the continuum breakup model. The

3D Gurney and DLV models can apply thin shell geometries and uses adjustment factors to account for larger grid resolutions in AECAT.

The ISO container material was steel, and different quantities of TNT were placed inside. In all cases, the TNT was centered on the floor of the ISO container. Figure 6 shows a cut plane for the 1/8 full test case, which used a TNT mass of about 7,500 kg. Additional loading densities are considered in [1].

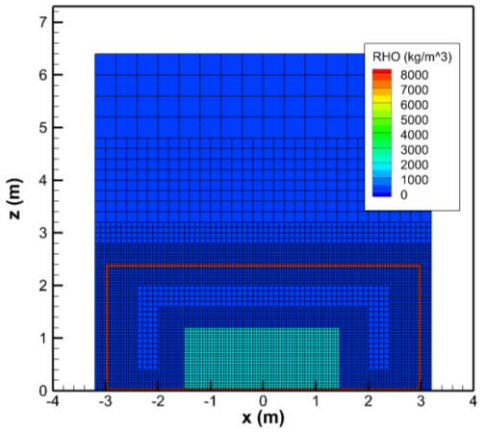

Figure 6. Cross-section of ISO container model: 1/8 full loading density.

The breakup of the ISO container was modeled using the continuum breakup, 3D Gurney and DLV models to predict initial debris velocities.

Figure 7 shows the predicted initial velocities for the DLV and 3D Gurney solvers for the full test case. The DLV is mostly uniform across the container surface and only varies with thickness near the corners. The velocity distribution from the Generalized 3D Gurney theory is not uniform as it includes the effects of the structure geometry, wall thickness and placement of the explosive.

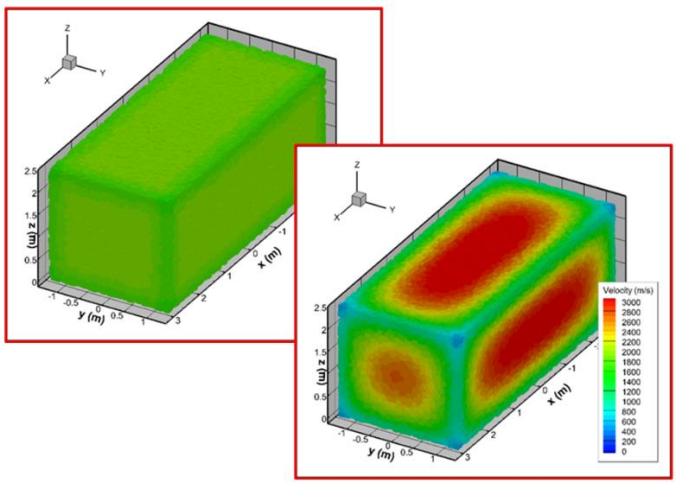

Figure 7. Initial fragment velocity contours for full test case: DLV (top left), GGT (bottom right).

The continuum breakup model uses strain-based criteria to turn an Eulerian representation of the steel material into Lagrangian fragments as the casing fails. The full detonation, casing expansion, and acceleration of fragments is modelled with this approach.

Therefore, there is not a straightforward "initial fragment velocity" for comparisons. Figure 8 shows the fragment velocities at 2 ms and 4 ms. The distribution in fragment velocity along the surface of the iso-container is very similar to the 3D Gurney model.

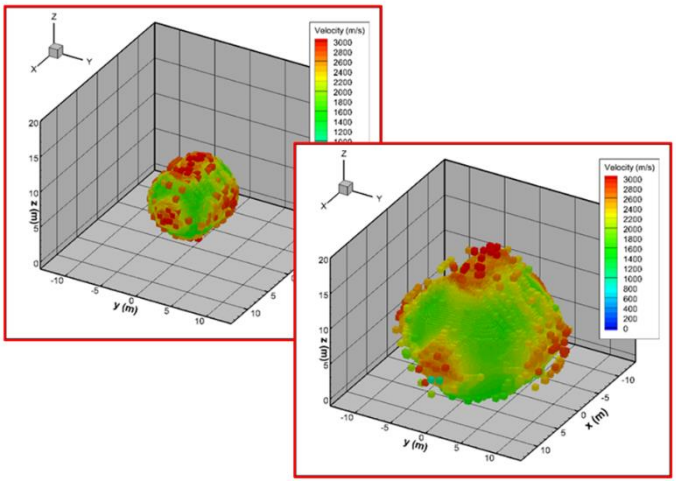

Figure 8. Instantaneous fragment velocity for continuum model for full test case: 2 ms (top left), 4 ms (bottom right).

Although the contour plots only depict the outermost fragments in the continuum model, they do not necessarily represent the entire magazine mass. Figure 9 compares the mass-averaged velocity for each model for various loading densities [1]. For the continuum breakup model, a mass-weighted average velocity of fragments as they were formed was taken. The mean velocity is consistent across all three models.

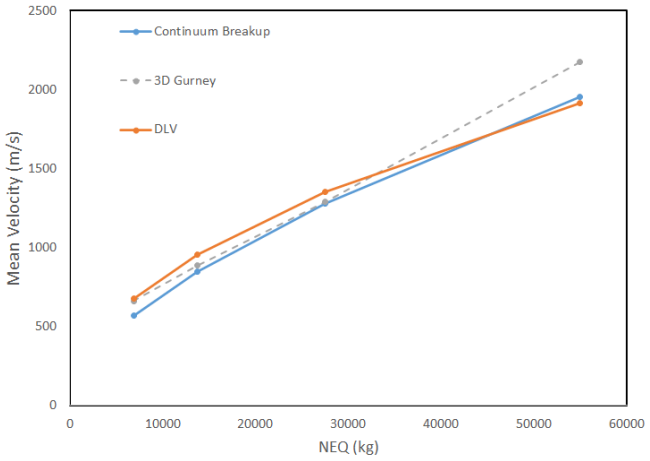

Figure 9. Mass-averaged velocity comparison for continuum, 3D Gurney and DLV models.

Accurate prediction of the fragment velocity distribution is important because it has a direct relationship to the strain rate of the structure as it expands during detonation. In turn, the structure strain rate directly affects the size of debris that are formed. In AECAT, the DLV and 3D Gurney models rely on the strain rate to provide a mean fragment size in conjunction with well-known Grady theory [36]. A three-dimensional Mott distribution is then applied. The continuum breakup model can predict sizes from Grady [36], or it may also employ a user specified size distribution, which generally needs to be

measured experimentally but could also be approximated using the same empirical laws.

Additional verification and validation studies are recommended for the modified GGT debris model. These studies should include multiple magazine geometries, wall thickness and explosive configurations. For lower packing densities, lower energy (i.e., lower strain and strain rate) breakup models are recommended to better predict the debris sizes.

Preliminary Validation

The purpose of the preliminary validation effort was to summarize an AECAT validation exercise using real-world experimental data. The data comes from the SciPan trials performed in collaboration between the United States Department of Defense and the U.S. Department of Defense Explosives Safety Board [42]. The trials examined the detonation of explosive material within light confinement magazine structures at low packing density. Experimental measurements were taken including standoff pressures, impulses, arrival times, as well as structure debris sizes and launch distances. These measurements were used as a preliminary validation of the AECAT software tool; in particular, data from the SciPan 4 trial was used which is described here.

Experimental Setup

The SciPan 4 experimental test site was the Upper Cactus Range of the Naval Air Warfare Center, Weapons Division in China Lake, California [42]. The elevation above sea level of the site is approximately 1525 m (5,000 ft), the temperature was 35°C, and the pressure was 102.066 kPa [42]. The test location was relatively flat extending 1000 m in all directions from the PES.

A schematic of the experimental configuration, including explosive, structure, and barricade, is shown in Figure 10. The single-compartment magazine structure dimensions were 9.1 m by 9.1m with ceiling height of 3.05 m. The magazine consisted of a floor slab, four walls and roof, all having different compositions and dimensions. The building materials and dimensions were representative of typical construction. The front wall and back wall were 7.5” (19.05 cm) reinforced concrete (R/C) with #16M rebar spaced at 40 cm. The third wall (counterclockwise from front) was 5.5” (14.0 cm) R/C with #16M rebar spaced at 40 cm, and the fourth wall was constructed from fully grouted, 8” (20.3 cm) concrete masonry units (CMU) with #16M rebar vertically spaced at 40 cm and #16M rebar horizontally spaced at 80 cm. The walls were not connected at the corners to isolate individual wall responses. The roof was comprised of a corrugated metal deck, R/C fill, and #10M rebar spaced 40 cm. The average thickness of the roof was approximately 11 cm (4.25”) and was supported with steel beams spanning the length of the structure. The floor slab was 4” (10 cm) R/C with #13M rebar spaced 40 cm.

The rebar was grade 60 steel with a yield strength of approximately 414 MPa, and the design strength of the concrete was stated as 20.7 MPa. Tests performed on the floor and walls showing compressive strengths of 27.0 MPa and 27.6 MPa, respectively. The front wall had a centered floor-to-ceiling door opening with a width and height of 3.0 m. A wire mesh and sand-filled barricade was located in the front of the structure with a height of 4.6 m and width of 9.1 m orientated at the door midline.

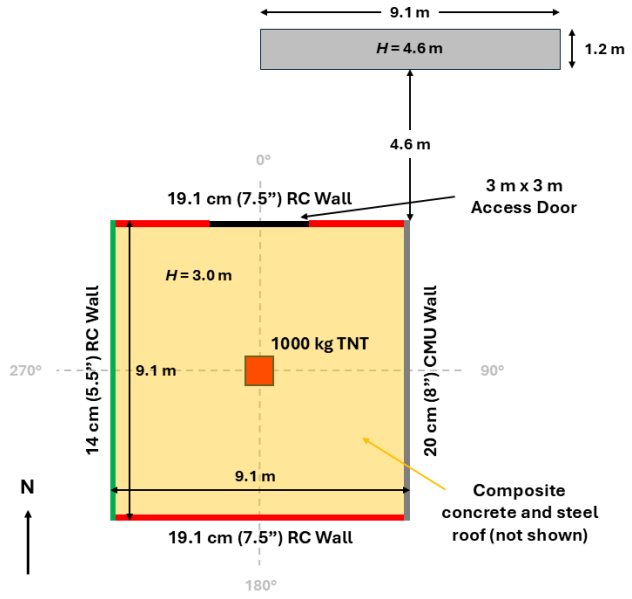

Figure 10. SciPan 4 structure and barricade schematic (adapted from *[42]*).

The explosive charge was comprised of 40 fiberboard boxes containing flaked TNT and weighing approximately 25 kg each. The boxes were stacked in a rectangular configuration and centered within the structure equidistant from each wall. The nominal NEQ of the stack was 1000 kg. Four C4 boosters and detonating cord was used to ensure complete detonation of the TNT.

Data collection was performed up to 1000 m from the magazine to analyze throw distances and debris sizes. Wall compositions were colored in order to differentiate between structure surfaces. Concrete and steel debris was collected and binned according to weight with lower cutoffs of 2 cm for concrete pieces and 1 cm for steel pieces.

Pressure transducers were used to measure the air blast along two radial lines extending from the center of the PES structure at 180 degrees (backwards) and 270 degrees (leftwards). The gauges were placed at radial distances of 15.2, 30.5, 45.7, 61.0, 91.4, 121.9, and 152.4 m.

Numerical Setup

AECAT Expert User Interface

The SciPan 4 trial was simulated using both the AECAT Expert and Virtual Globe User Interfaces. The explosive charge was modelled using a simplified cubic shape of length 0.855 m and initialized using a balloon analogue model of high-pressure TNT detonation products, which captures the energy release of the detonation without explicitly modelling it in the simulation. The PES structure was imported into AECAT as a triangulated surface mesh model with each side, roof and floor slab having unique component numbers, as shown in Figure 11. Each structural component was defined using a concrete material model and a specified thickness corresponding the documented experimental wall thickness values. The TNT block model was positioned in the center of magazine structure on the floor.

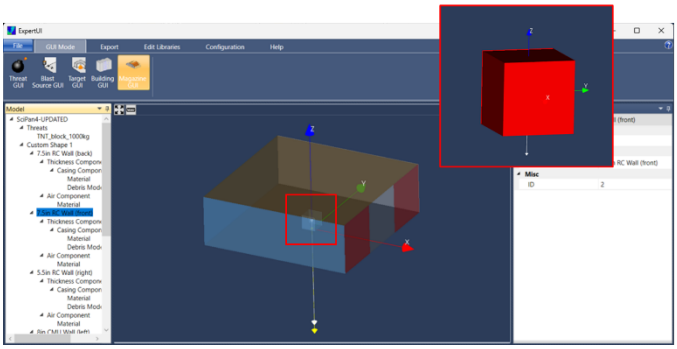

Figure 11. Creation of SciPan4 PES in AECAT Magazine GUI.

The Fast Fragmentation modelling approach was used to calculate the structure debris breakup, employing the modified generalized 3D Gurney model for initial debris velocities. This provides additional modelling fidelity of the spatial distribution of explosive energy exerted on the magazine structure over the previous validation efforts which employed the Debris Launch Velocity (DLV) model. In order to accelerate convergence of the Gurney solver, a default overrelaxation value of 2.0 was used.

The Grady model was used to predict localized mean debris sizes on each of the wall surfaces based on local strain rates. A 3D Mott distribution was used to represent the overall size distributions. Two improvements were made over previous validation efforts: 1) the strain and strain rate definitions for building geometries have been improved to better represent the failing motion, and 2) a cell-based debris initialization methodology has been developed that uses a group Lagrangian approach to more accurately represent localized fragment/debris size distributions during initialization.

Table 1 summarizes the material properties defined for the concrete walls.

Table 1. AECAT material properties for concrete used for validation study.

Elastic Modulus, E (GPa)	30.0
Fracture toughness, K_c (MPa-$m^{0.5}$)	0.8
Specific heat, C_p (J-kg/K)	750.0
Failure Strain Factor, FSF	1.0
Density, ρ (kg/m^3)	2400
Thermal Diffusion Coefficient (m^2/s)	1.0 x 10^{-6}
Thermal Softening Coefficient (1/K)	1.0 x 10^{-3}
Plastic Flow Stress, Y (MPa)	4

Although the experimental concrete walls were reinforced, AECAT employed a simplified pure concrete modelling approach. This simplification is not expected to have a large impact on the results for two reasons. First, the walls are failing in tensile loading, in which concrete and reinforced concrete have similar structural properties. Second, the reinforced rebar is positioned sufficiently far apart as to not limit the sizes of the debris formation. No comparisons are made to rebar debris collection.

The CMU wall was constructed using cement blocks (the type was not specified) which are typically hollow. The gaps in the blocks were fully filled with grout, which itself has a wide range of material properties, different to those of the concrete, depending on the type used. In order to better represent the reduced strength and increased ductility of CMU walls, the modulus of elasticity for the CMU wall was reduced to 10.0 GPa; however, improved representation of complex composite materials should be investigated in future work.

In the experiment the roof of the PES was supported by steel beams spanning the length of the structure. A corrugated metal deck was placed on top of these steel beams and the reinforced concrete on top of it. The roof structure was also modeled as a solid concrete surface without the corrugated metal component. Due to the significant effect that this metal under piece would have on the energy transfer and breakup of the roof, the debris from the roof was omitted from the size distribution comparison plots.

AECAT Virtual Globe User Interface

The explosive blast and magazine debris throw was simulated in the Virtual Globe User Interface at the experimental test site, as shown in Figure 12. The magazine and barricade were imported into the same location as the experimental test site using the Virtual Globe GUI, centered at coordinates of 36.1194153 deg. latitude, -117.812334 deg. longitude. The barricade was modeled as a rigid structure to with respect to the blast and fragment/debris throw, but was not included in the magazine breakup or debris field. Numerical gauge points were placed along the same directions and radial distances as experimental pressure sensors, also shown in Figure 12.

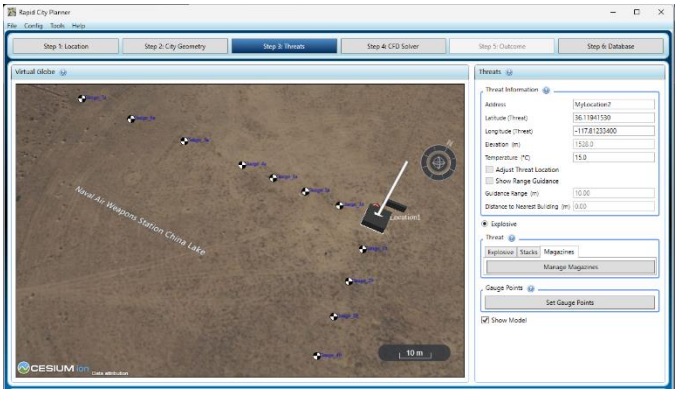

Figure 12. Setup of simulation in AECAT Virtual Globe, showing location of PES, barricade, and monitor points.

A simulation end time of 2 seconds was defined which is sufficient for the blast wave to travel past the sensor locations and the debris travel sufficiently far to hit a 15 J minimum kinetic energy cutoff value. A minimum CFD cell size of 2.7 cm and a maximum cell count of 2 million was used for the blast calculation. The documented atmospheric conditions of the experiment were 102.066 kPa and 308.25 K, while AECAT employed simplified standard atmospheric conditions of 101.325 kPa and 300 K.

The brittle equivalent bare charge (EBC) model in AECAT was employed for concrete which produced an effective charge mass of roughly 404 kg. This EBC value was predicted based on the original NEQ and magazine structure mass to account for the acceleration of the concrete debris. The scaled hemispherical surface blast model was used to initialize the equivalent charge; thus detailed detonation of the TNT stack was not modeled.

The debris was modeled using the tumbling fragment shape and drag models in AECAT. Five permutations were used which is generally

sufficient for statistical convergence given the large number of debris pieces associated with magazine breakup. A total of 100,000 representative group-Lagrangian fragment groups were used to represent each wall for statistical convergence. This group-Lagrangian approach employed the new cell-based fragment/debris mapping model for better representation of local Mott-based debris size distributions. Fragments under 1.5 cm were ignored from the calculation, as this was the lower limit on debris collection in the experiment [42].

The terrain surface was defined as a reflective boundary with a coefficient of friction of 0.5 and coefficient of restitution of 0.4; both are representative for concrete reflection off a hard soil surface. A secondary breakup model was employed to represent subsequent shattering of concrete debris during ground ricochets. The model enforced brittle debris breakup. The terrain was modelled as a rigid surface in Rapid City Planner, and therefore the crater formation and associated energy losses were not considered.

Results

Gauge point comparisons were made with experimental measurements in terms of peak overpressure, peak impulse and blast wave arrival times. The comparisons were made up to a distance of 150 m, or scaled distance of roughly 15 m/kg$^{1/3}$, and are shown in Figure 13-Figure 15. AECAT predictions for an open hemispherical surface burst of the same magnitude are also included in the figure. Further, the comparisons include BEC model predictions for an Above Ground Structure and an open hemispherical surface burst. For the experimental measurements, the blast results are included along the 180 and 270 degree directions. However, directionality effects are not captured in the BEC model or AECAT's fast magazine blast modelling approach. The numerical predictions from both models match the experimental peak pressures and impulses reasonably well; however, the AECAT predictions underpredict the peak pressure in the far field due to larger cell sizes and excessive coarsening in the AECAT fast modelling approach. The presence of the structure increases the experimental blast arrival time in the near field which is not picked up by the model predictions; however, the blast attenuation effect has relatively little significance on the arrival time prediction at larger distances.

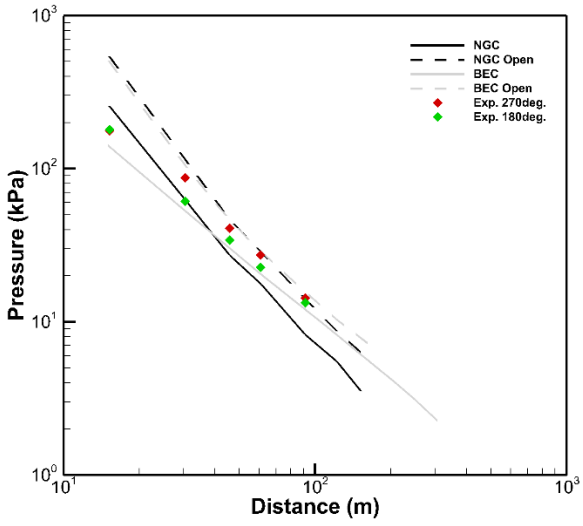

Figure 13. Gauge point comparisons of peak overpressure for AECAT, experimental measurements [42]*, and the BEC model* [42].

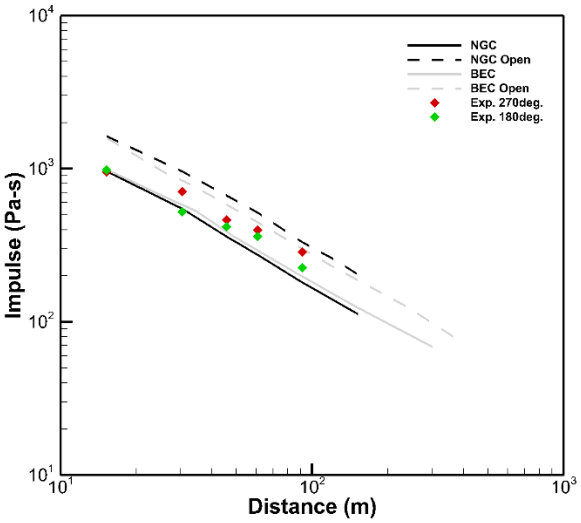

Figure 14. Gauge point comparisons of peak impulse for AECAT, experimental measurements [42]*, and the BEC model* [42].

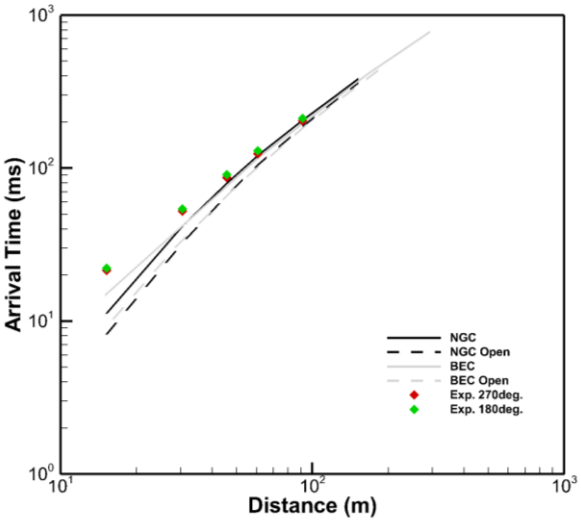

Figure 15. Gauge point comparisons of blast arrival time for AECAT, experimental measurements [42]*, and the BEC model* [42].

Following detonation of the explosive TNT stack, debris from the PES was collected and recorded experimentally. Each piece of debris was flagged in its final resting place, and its mass was recorded. Colored pigments were used to denote each wall of the PES. Debris collection is not an exact science, and difficulties observed in the collection process are explained in [42].

Figure 16 plots 500 random trajectory lines of debris in AECAT showing the concrete pieces ricochet off the terrain surface and lose momentum. The analysis was performed with secondary breakup (shattering) model employed to incorporate the effects of this phenomenon.

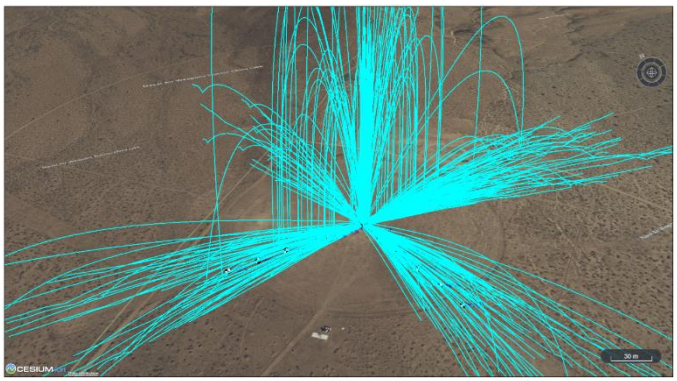

Figure 16. AECAT trajectory line plot for 500 random concrete debris pieces.

Figure 17 plots the numerical fragment count on top of the flagged experimental debris pieces, which is meant solely to show a reasonable qualitative comparison of the debris throw. Firstly, the numerical and experimental debris is thrown primarily in the normal directions to the wall surfaces, and the throw angle is in good agreement. Debris is thrown from the corners of the structure also but in lesser quantities observed both experimentally and numerically. Secondly, the effects of the barricade are seen numerically and experimentally with the reduced fragment count between 15 and 45 degrees on the right side of the door opening compared to the left side (between 315 and 345 degrees). Finally, both experimental and numerical show the venting effects of the door which reduce the impulsive loading on that PES wall reducing initial debris velocities and corresponding debris distances in that direction. Figure 17 shows the numerical fragment count with consideration of debris shattering, which results in larger fragment counts with outward directionality.

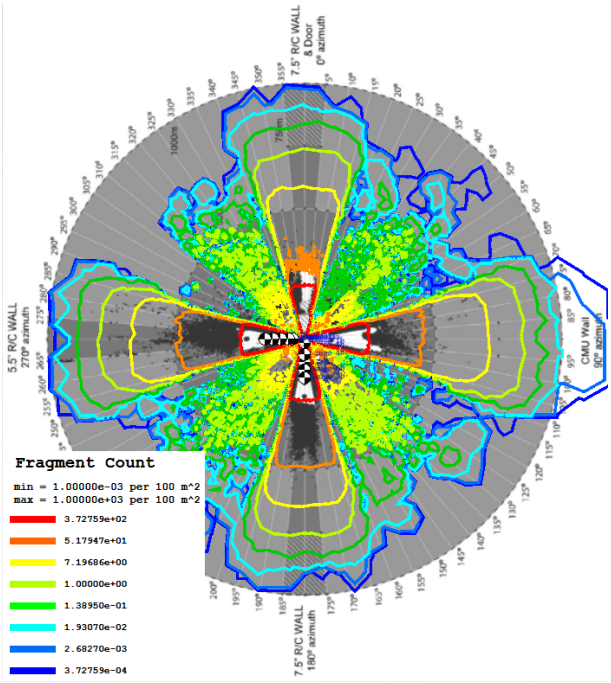

Figure 17. AECAT terrain contour of fragment count plotted over experimental debris collection scatter plot [42].

Figure 18 plots the experimental Inhabited Building Distance (IBD) in grey which is defined as the area within which the lethal fragment count is less than 1 per 55.7 m^2, and a hazardous fragment is defined as a fragment with an impact kinetic energy of at least 79 J. Since the impact kinetic energy was not measured experimentally, a fragment mass of 90 grams was chosen instead which corresponds to a piece of concrete debris shaped roughly as a sphere falling at a terminal velocity. Since this quantity is not output by AECAT, Figure 18 overlays the numerically predicted probability of fatality which is based on the lethality of fragments and the likelihood of them hitting a standing 2-m tall human. Although this comparison is not "apples-to-apples", the 10% fatality is generally in good agreement with the experimentally measured IBD line. The figure shows the numerical fatality predictions with consideration of debris shattering. When shattering is modelled, the lower fatality extents (1-10% fatality) were observed to increase by 50-100 m in the outer regions due to an increased number of debris pieces. In the near field, where the probability of fatality is high, the effects are less significant and may even have a reduction effect on fatality due to reduced debris sizes.

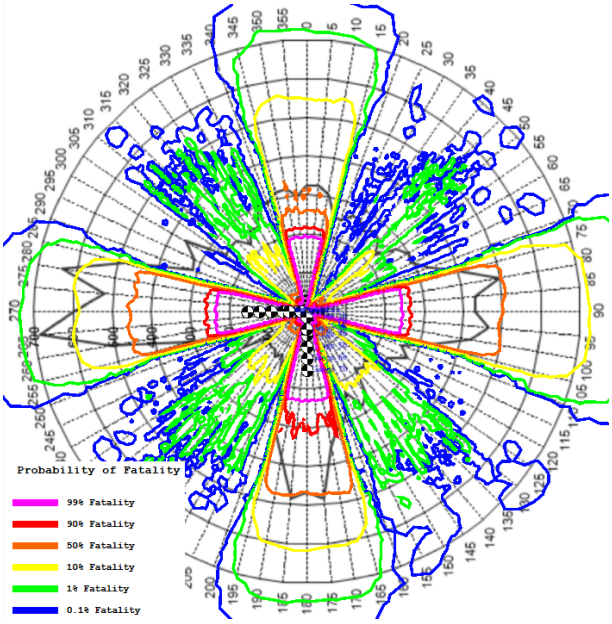

Figure 18. AECAT terrain contour of fatality probability plotted over experimental debris IBD (in grey) [42].

Along with flagging the pieces of debris during the experimental collection, the debris sizes were recorded for each wall. Due to experimental challenges during data collection [42], the measured debris size distributions may not perfectly represent all debris but should be representative. Alternatively, AECAT tracks all debris pieces allowing for detailed representation of the full structure as well as individual wall components. Figure 19 compares the experimental and numerical size distributions for each wall. The numerical results are shown with and without the consideration of secondary breakup, showing the large reduction in size during ground shattering. The numerical predictions match well with the experiments when shattering is considered which has a substantial effect on the size distribution of each wall. During experimental debris collection, the shattered concrete pieces were stuck back together and recorded as one in the far field where secondary breakup was obvious. For that reason, the larger 10% of fragment sizes, which would be thrown farther outwards, are under predicted numerically. Interestingly, these larger 10% of sizes are better predicted when secondary debris is not considered.

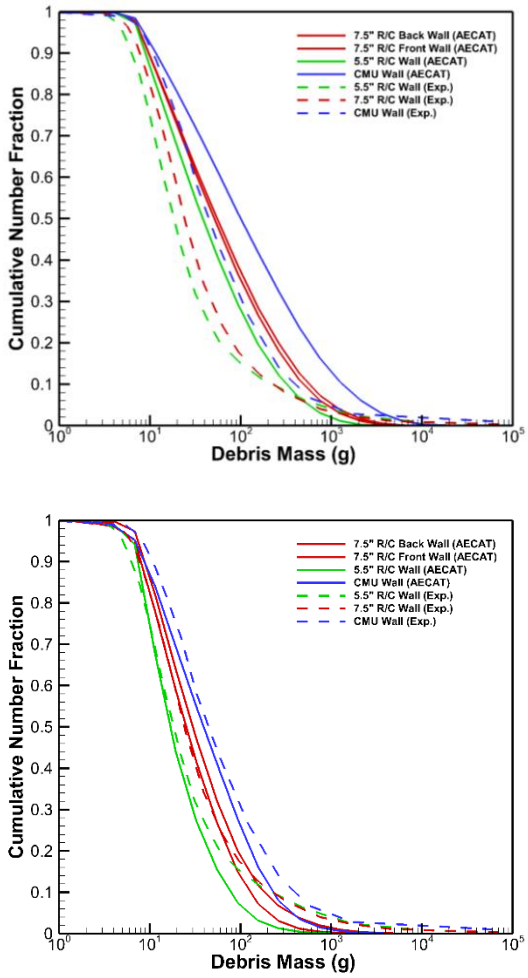

Figure 19. Debris size distributions for AECAT, experimental measurements [42]. *Before shattering (top), after shattering (bottom).*

The roof has been omitted from the analysis due to uncertainty surrounding the experimental collection. It was stated that the wind carried the upward thrown roof debris towards the north/northwest direction where the terrain was particularly hard. This led to much greater shattering of the roof segments into numerous small pieces, and thus it was decided experimentally to not collect roof debris in that vicinity due the inevitable high likelihood of fatality. Numerically, the roof debris sizes were similar to the walls prior to shattering, but they experienced much higher reductions in sizes during ground impact due to their high altitude and normal impact direction. Without consideration of these highly shattered pieces in the experimental collection, the experimental results are skewed towards larger unshattered segments and do not provide a realistic comparison to AECAT predictions. Finally, it is worth noting that the corrugated metal component under the concrete roof section may also influence behavior by absorbing initial impulsive loading.

Enhancements for Naval Storage Scenarios

The existing AECAT capability for modelling blast, fragmentation, and debris throw effects from stored ammunition and explosives for land-based scenarios has been extended for basic naval storage applications. Several enhancements have been made to the AECAT system to support consequence analysis of storage scenarios upon naval vessels and multi-compartment magazine structures. This initial naval storage capability is built upon the previously developed land-based approaches for modelling blast, fragmentation, and debris throw effects, as described previously in this work and in [1].

Ship and multi-compartment storage geometries are imported into the AECAT Expert User Interface as triangulated 3D surface models. The thickness and composition of the walls and interior compartments are defined by the user in the same way as for magazines. Likewise, munitions/stacks are imported and placed within a ship compartment, as shown in Figure 20.

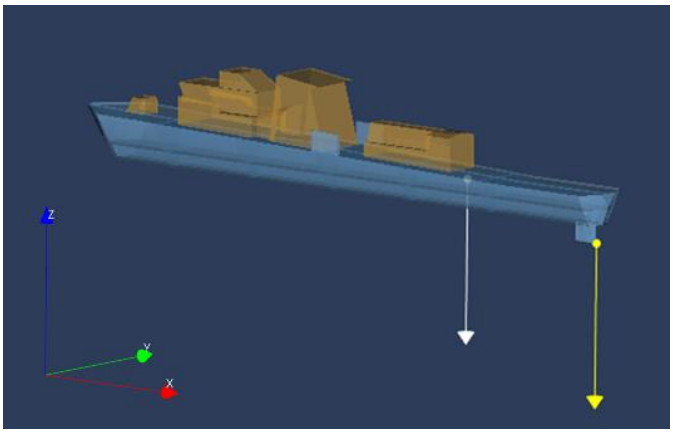

Figure 20. Transparent ship hull for an example geometry used for accurate threat placement.

Once the ship and threat quantities are defined, the same steps are employed to run/export the “magazine” to the database for consequence analysis in a real-world environment, including the calculation of debris for Fast Fragmentation modelling.

The AECAT Virtual Globe methodology is also equivalent for ships as for land-based magazines; however, vertical displacement is specified to set the ship draft placing the ship hull below the water (e.g., terrain) surface. Fragments and debris below the water surface are not currently considered in the analysis.

Both fast and detailed methodologies can be employed for naval ship storage; however, the detailed approach is currently recommended and is being used to inform on fast modelling approaches and methodologies.

Several improvements to the magazine modelling approaches have been recently added to the AECAT system to accommodate naval ship and multi-compartment scenarios, including:

- Normal vector corrections – The Gurney solver traditionally relies on wall normal directions, with initiation position effects applied, assuming outward debris throw. For complex multi-compartment scenarios, special treatment has been added to define outward directions relative to the explosive position.
- Stability improvements for Gurney solver – Stability methods were added to the fast fragmentation Gurney solver in terms of 1st order explosive/air-structure interface treatment to improve robustness for complex structures.
- Localized strain rates for debris size prediction – Single munitions and stacks traditionally use a global strain rate

approximation when predicting fragment sizes, which can be an inaccurate approximation for magazines/ship debris (especially multi-compartment facilities) where the strain rate varies substantially across the structure.

- Low strain debris prediction – Munitions traditionally use Grady theory to predict mean fragment/debris sizes which has no lower limitation on strain rate (i.e., very large sizes predicted). Magazines and multi-compartment ships can experience low strain breakup, and thus a Glen-Chudnovsky variation can be employed.

Naval storage demonstration scenario

To demonstrate the naval ship storage developments in AECAT, a Royal Canadian Navy (RCN) City-class frigate has been modeled in the Halifax Harbour in Nova Scotia as a hypothetical case study. This demonstration is intended as a verification and not a validation study; the purpose is to demonstrate the initial capabilities and to highlight differences between the fast and detailed modelling approaches. Future work will be focused on full validation of the naval storage modelling capability.

The demonstration scenario consisted of an arbitrary explosive quantity – 20,000 kg block of uncased TNT explosive – stored in an outside compartment on the aft portside of the naval vessel. The structure model of the City-class frigate consisted of both an external definition of the geometry as well as internal storage compartments with bulkheads and ship superstructure. For model simplicity the ship material was defined as steel with a uniform thickness of 1 cm. A schematic of the vessel from AECAT is shown in Figure 21.

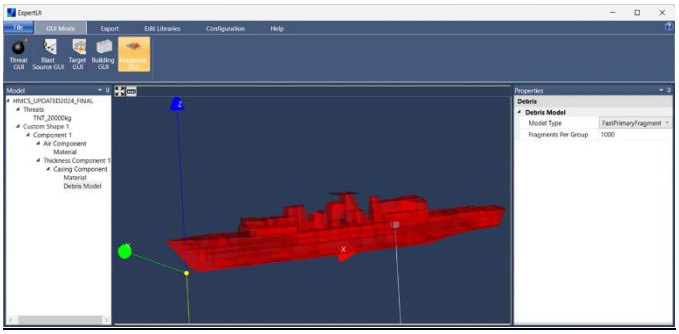

Figure 21. RCN City-class frigate with explosive location indicated by yellow circle.

For the detailed modelling approach, 400 tracer particles were used to track the displacement of the ship walls, and a displacement criteria of 2 m was used for continuum breakup (i.e., conversion of the Eulerian steel material to discrete Lagrangian steel particles). Grady theory was used to predict the mean size of the debris based on local strain rates for both solvers (i.e., fast and detailed).

Figure 22 shows the initial debris velocity field predicted by the fast fragmentation generalized 3D Gurney approach, while Figure 23 shows the debris velocities using the detailed modelling approach at 3 ms and 11 ms after detonation. The detailed modelling approach predicts much larger localized velocities near the explosive event and lower velocities farther from the blast. This does not appear to be accurately captured well by the fast modelling approach which assumes the entire ship breaks up during an explosive event. The fast modelling approach does capture local effects to some extent; however, this does not appear to be sufficiently well captured for complex multi compartment structures, and more efforts are recommended to improve accuracy.

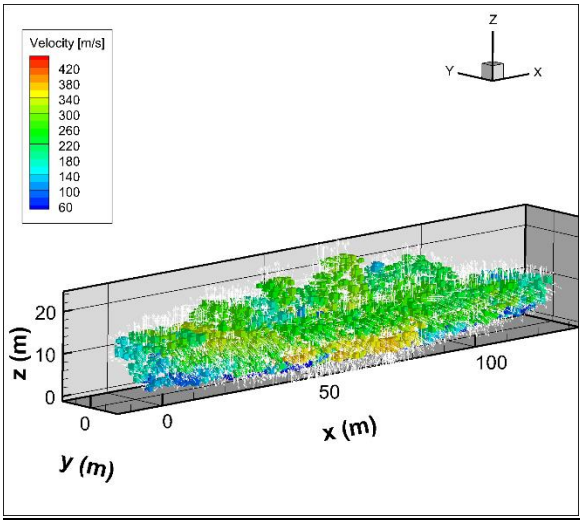

Figure 22. Initial debris velocity field using fast debris solver.

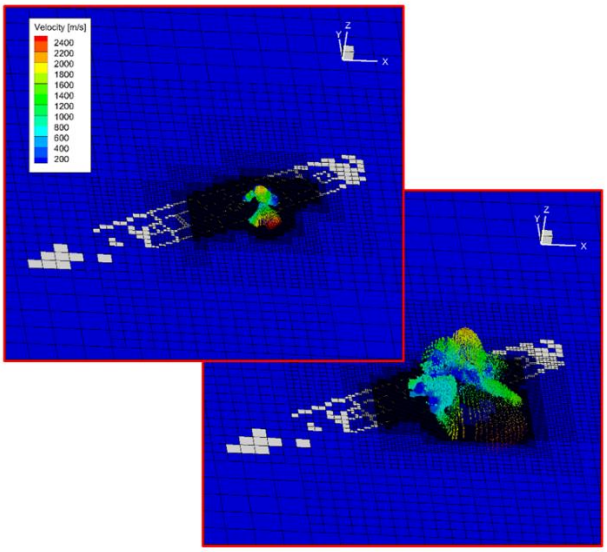

Figure 23. Debris velocity prediction using detailed modelling approach at 3 ms (top) and 11 ms (bottom) after detonation.

The fast and detailed ship models were both placed in the AECAT Virtual Globe User Interface on the Halifax waterfront, and lowered vertically into the water for a 5 m draft. This resulted in the storage compartment containing the TNT explosive being positioned above the water surface. For this analysis the water surface was treated as a rigid reflecting surface, and debris initialized below the water surface was not included in the simulation or outcomes.

Figure 24 shows the probability of fatality contours for the fast and detailed modelling approaches, while Figure 25 compares the 1% fatality line to the DFD6 QD (IBD) level. The fatality contours are more evenly distributed around the perimeter of the ship for the fast-modelling approach, whereas the detailed approach shows very localized extremes near the TNT storage compartment and very directional effects that were influenced by the internal ship

compartments and complexities in geometries. Both approaches incorporate influences of the coastal terrain and urban building geometries, including reflections and shielding.

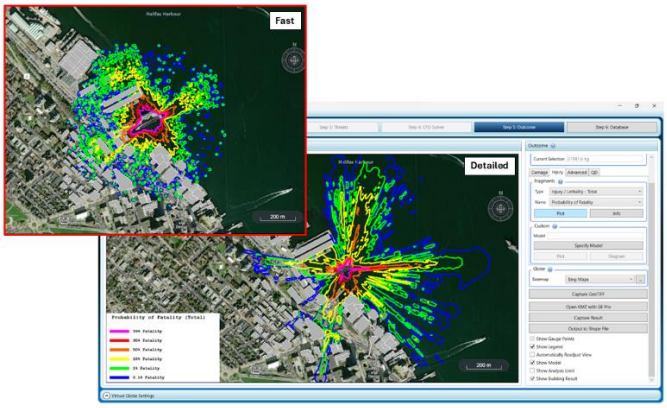

Figure 24. Contours of probability of fatality for fast (above) and detailed (below) modelling approaches.

Figure 25. DFD6 (IBD) QD outcome compared with 1% fatality isoline for fast (above) and detailed (below) modelling approaches.

Figure 26 shows a pressure contour for the detailed modelling approach on the horizontal plane cut through the center of the TNT block at 1 ms and 5 ms after detonation. The blast wave can be seen channelling within ship compartments and increasing on compartment walls due to confinement before wall failure. Velocity vectors are included in the figures to show the high directionality of the blast wave propagation. Figure 27 shows the same contour map at 3 ms and 12 ms overlaid with the debris throw. The debris scatter points are scaled with their predicted sizes, showing small debris sizes on the front wall near the blast where strain rates are very high and larger debris pieces farther from the blast.

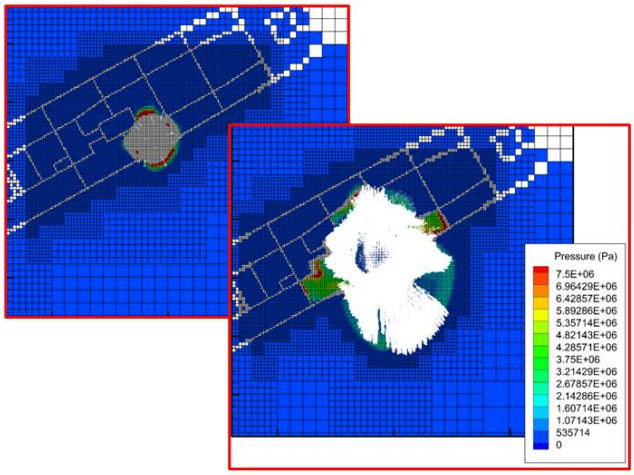

Figure 26. Contours of pressure along horizontal plane through centre of TNT block at 1 ms (top) and 5 ms (bottom) after detonation. Velocity vectors shown in white.

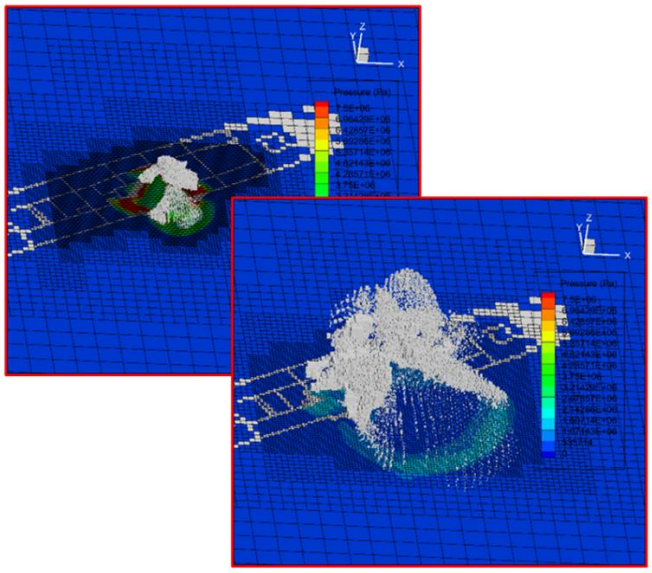

Figure 27. Contours of pressure along horizontal plane through centre of TNT block at 3 ms (top) and 12 ms (bottom) after detonation. Debris scatter sizes shown in white.

Conclusions and Future Work

The AECAT software tool, introduced previously in [1], was summarized in this work, including an overview of the established RCP modelling platform upon which it is based and an example scenario of the historical Halifax Explosion of 1917. The AECAT system is primarily intended to support risk-based licensing operations and inform on consequences of explosive events in land- and naval-based storage environments. The system is based on first-principles CFD technology and uses physics-based modelling approaches to simulate explosive events in 3D while inherently incorporating effects of natural terrain and site infrastructure including buildings and barricades.

The development and integration of the AECAT system into the RCP platform has been underway for nearly five years, with an initial

focus on establishing a software framework to support risk-based licensing operations and consequence analyses for storage scenarios through established numerical methods and QD-based outcomes, as well as significant modelling developments to consider stacked A&E items and light- and heavy-confinement storage structure breakup and debris. Recent focus has included expanding the system to consider more complex naval storage scenarios, system usability improvements, and model validation.

Validation of existing modelling approaches remains a primary focus of the development programme. Preliminary validation for SciPan 4 was presented in this work, however, additional validation for storage magazines and earth-covered storage scenarios in particular is recommended. Several planned validation and predictive modelling exercises are planned in the future, including for MERCURY 10 trials in USA (2025), Singapore heavy earth-covered magazine trials (planned 2027), and German NATO standard ECM 146 trials (planned 2028). Validation opportunities for naval scenarios are currently being investigated.

Development and testing of naval and multi-compartment magazine models (both fast and detailed) is currently in progress. Verification of naval scenarios has been completed and tested in a variety of scenarios in Canadian-based real-world environments. Additional testing and adaptation of the modelling approaches is recommended, including improvements to the fast modelling approach to account for propagation between compartments, successive failure of adjacent volumes, and sympathetic detonation.

Future developments planned for the AECAT programme include further support for risk analyses, including measures of event likelihoods, to inform on complex and/or marginal storage scenarios, as well as expanding the GIS-based system to facilitate standard siting and licensing activities.

References

[1] N. J. McCormick, S. D. Ryan and D. R. Whitehouse, "Ammunition and Explosives Consequence Analysis Tool (AECAT) to Support Risk Assessment of Storage-Based Explosive Scenarios," in *PARARI 2022 Australian Explosive Ordnance Safety Symposium*, Canberra, Australia, 2022.

[2] R. C. Ripley, F. Zhang, C. T. Cloney, S. McClennan and N. J. McCormick, "A Modern Blast Solver Strategy and Its Urban Application," *DRDC-RDDC-2016-P044,* 2016.

[3] R. C. Ripley, "Rapid City Planner 2 Final Report," Martec Limited, TR-19-82, Halifax, NS, 2019.

[4] F. Zhang, "Confined Heterogeneous Blast," in *Military Aspects of Blast and Shock (MABS)*, Calgary, AB, 2006.

[5] R. C. Ripley, C. T. Cloney, L. Donahue and F. Zhang, "Extended Near-Field Regime in Urban Confinement," in *Military Aspects of Blast and Shock (MABS)*, Bourges, France, 2012.

[6] R. C. Ripley, L. Donahue and F. Zhang, "Fragmentation of metal particles during heterogeneous explosion," *Shock Waves,* vol. 25, no. 2, pp. 151-167, 2015.

[7] L. Donahue, F. Zhang and R. C. Ripley, "Numerical Models for Afterburning of TNT Detonation Products in Air," *Shock Waves,* vol. 23, no. 6, pp. 559-573, 2013.

[8] F. Zhang, K. Gerrard and R. C. Ripley, "Reaction Mechanism of Aluminum-Particle-Air Detonation," *Journal of Propulsion and Power,* vol. 25, no. 4, pp. 845-858, 2009.

[9] S. Ryan, N. McCormick and R. Ripley, "Blast and Fragmentation Modelling in Urban Environments using Rapid City Planner," *Shock Waves,* 2025.

[10] H. Ji and F. S. Lien, "Speedup Methods of the High-Speed Compressible Multiphase Solver," WATCFD Technical Report, Waterloo, ON, 2018.

[11] R. Mittal and G. Iaccarino, "Immersed Boundary Methods," *Annu. Rev. Fluid Mech.,* vol. 37, no. 239, 2005.

[12] N. J. McCormick, R. C. Ripley and F. Zhang, "Double-Sided Immersed Boundary Method with Thin-Shell Structures for Fast Blast Simulation," in *Military Aspects of Blast and Shock (MABS)*, The Hague, The Netherlands, 2018.

[13] R. Ripley, N. McCormick, L. Donahue and F. Zhang, "Application of Rapid City Planner to Historical World Explosion Events," in *25th Military Aspects of Blast And Shock Symposium*, The Hague, The Netherlands, 2018.

[14] D. Baingo, "The Halifax Harbour Explosion Today: Rapid City Planner," 8th Annual Disaster Risk Reduction Roundtable, DRDC, 2017.

[15] N. B. o. I. Underwriters, "Plan Showing Devastated Area of Halifax City, N.S.," Nova Scotia Archives V6/240 - 1917 Halifax loc.4.2.3.2 / negative: O/S N-111, Halifax, NS, 1918.

[16] G. Kinney, Explosive Shocks in Air, New York: Second Edition, Springer-Verlag, 1985.

[17] Federal Emergency Management Agency, "FEMA 426 - Reference Manual to Mitigate Potential Terrorist Attacks Against Buildings," FEMA, 2003.

[18] Bowen, Fletcher and Richmond, "Estimate of Man's Tolerance to the Direct Effects of Air Blast," Defense Atomic Support Agency DASA-2113, 1968.

[19] Godfrey, Sydenstricker, Ong, Burke and Malebranche, "Human Injury Information System Concept Exploration," Armstrong Laboratory - USAF, Report No. AL/YA-TR-1994-0050, JTCG/AS-92-D-006, 1994.

[20] Department of Defence Unified Facilities Criteria, "Structures to Resist the Effects of Accidental Explosions," UFC 3-340-02.

[21] North Atlantic Treaty Organization, "AASTP-1 NATO Guidelines for the Storage of Military Ammunition and Explosives Edition C Version 1," NATO Standardization Office (NSO), 2023.

[22] T. Zaker, "Fragment and Debris Hazards," Washington, D.C., 1975.

[23] J. Starkenberg, K. J. Benjamin and R. B. Frey, "Predicting Fragmentation Propagation Probabilities for Ammunition Stacks," ARL-TR-949, U.S. Army Research Laboratory, Aberdeen Proving Ground, MD, 1996.

[24] M. Crull and W. Shannon, "A Summary of the Fragmentation Hazard Study Phase III: Fragment Hazards from Detonation of Multiple Munitions in Open Stores," CEHNC-EDS-O-12-07, 2012.

[25] M. Crull and W. Shannon, "Historical Testing and Analysis of Stacks of 155 mm Projectiles: Fragment Mass Distribution and Initial Fragment Velocities," CEHNC-EDS-O-13-01, 2013.

[26] E. Draper and R. Watson, "Collated Data on Fragments from Stacks of High Explosive Projectiles," MOD TM 2/70, 1970.

[27] M. Crull and S. Hamilton, "Methodologies for Calculating Primary Fragment Characteristics," DDESB Technical Paper 16, Revision 5, Huntsville, AL, 2016.

[28] D. Feinstein, "Fragment Hazard Study: Grading and Analysis of 155-mm Yuma Test Fragments," Final Report, Contract DAAB09-72-C-0051, 1972.

[29] F. Weals, "ESKIMO I. Magazine Separation Test," NWC TP 5430, 1973.

[30] D. Feinstein and H. Nagaoka, "Fragment Hazards from Detonation of Multiple Munitions in Open Stores," Final Report, Phase III, Contract DAHCO4-69-0056, 1971.

[31] S. Jacobs, "The Gurney Formula: Variations on a Theme by Lagrange," NOLTR 74-86, 1974.

[32] R. Ramsey, J. Powell and W. Smith, "Fragment Hazard Investigation Program," NSWC/DL TR-3664, 1978.

[33] J. Powell, W. Smith and F. McCleskey, "Fragment Hazard Investigation Program: Natural Communication Detonation of 155-mm Projectiles," NSWC TR 81-54, 1981.

[34] "Manual of NATO Safety Principles for the Storage of Military Ammunition and Explosives," AASTP-1, 2010.

[35] R. Ripley, "Numerical modeling of structural reactive material casings," Halifax, 2016.

[36] D. Grady, Fragmentation of Rings and Shells: The Legacy of N.F. Mott, Berlin: Springer, 2006.

[37] E. Rottenkolber and W. Arnold, "A generalization of the Gurney formalizm to three dimensions," in *The 21st International Symposium on Ballistics*, Adelaide, Australia, 2004.

[38] A. Dorr, K. Michael and G. Gurke, "Experimental investigations of the debris launch velocity from internally overloaded concrete structures," 2002.

[39] J. van Doormall, A. Door and R. Forsen, "Debris launch velocity program DLV," in *The 11th International Symposium on the Interaction of the Effects of Munitions with Structures ISIEMS*, 2003.

[40] P. Kummer, "Debris throw from magazine walls due to explosions, debris, launch angle," 2006.

[41] M. van der Voort, F. Radtke, Y. van Amelsfort, Y. Khloe, I. Stacke and M. Voss, "Recent developments of the KG software," in *The 34th DoD Explosives Safety Seminar, DDSEB*, Portland, USA, 2010.

[42] R. Conway, J. Tatom and M. Swisdak, "SciPan 4 Program Description and Data Summary," Naval Facilities Engineering Command. Engineering and Expenditionary Warfare Center. Technical Report TR-NAVFAC EXWC-CI-1306., 2013.

Contact Information

Neil McCormick, M.A.Sc., P.Eng.
Work phone: +1 (902) 417-2500 Ext. 2491
e-mail: neil.mccormick@lr.org

Acknowledgments

The authors acknowledge the funding provided by the Government of Canada Department of National Defence (DND) Director of Ammunition and Explosives Regulation (DAER) for the initial phases of the AECAT development programme.

Definitions/Abbreviations

A&E	Ammunition and explosives

AASTP	Allied Ammunition Storage and Transport Publication
AECAT	Ammunition and Explosives Consequence Analysis Tool
ASL	Above sea level
CFD	Computational fluid dynamics
CMU	Concrete masonry units
DAER	Director Ammunition and Explosives Regulation
DDESB	Department of Defense Explosives Safety Board
DEM	Digital elevation model
DFD	Debris and fragment distance
DLV	Debris Launch Velocity
DND	Department of National Defence (Canada)
DRDC	Defence Research and Development Canada
EBC	Equivalent bare charge
ECM	Earth-covered magazine
EOS	Equation of state
ES	Exposed site
EWD	Explosives Workshop Distance
GGT	Generalized Gurney Theory
GIS	Geographic Information System
GUI	Graphical User Interface
HD	Hazard division
HFD	Hazardous Fragment Distance
IBD	Inhabited Building Distance
IBM	Immersed boundary method
IMD	Inter-Magazine Distance
M&S	Modelling and Simulation
MFD	Maximum Fragment Distance
NEQ	Net Explosive Quantity
PES	Potential Explosion Site
QD	Quantity-distance
RC	Reinforced concrete
RCN	Royal Canadian Navy
RCP	Rapid City Planner